ELSEVIER

Catalysis Today 68 (2001) 11–20

CATALYSIS TODAY

www.elsevier.com/locate/cattod

Comparison of disordered mesoporous aluminosilicates with highly ordered Al-MCM-41 on stability, acidity and catalytic activity

Dongyuan Zhao*, Cong Nie, Yaming Zhou, Shijing Xia, Limin Huang, Quanzhi Li

Department of Chemistry, Fudan University, Shanghai 200433, PR China

Abstract

A simple procedure has been described to directly synthesize hydrothermally stable, disordered mesoporous aluminosilicate materials with strong surface acidity by using a polymer aluminosilicate precursor, and cationic surfactant cetyltrimethylammonium bromide (CTAB) as the structure-directing agent. The comparison of stability, acidity and catalytic activity for the disordered mesoporous materials and Al-MCM-41 has been studied by X-ray diffraction (XRD), transmission electron microscopy (TEM), N_2 adsorption/desorption, infrared spectra, NH_3-temperature program desorption (NH_3-TPD) and ^{27}Al MAS NMR techniques. The results show that the disordered mesoporous materials are very similar to mesoporous material MCM-41 as regards its uniform mesopore sizes at the mean value of 3.0 nm, while the mesoporous channel arrangement is fully disordered similar to that for KIT-1 prepared by the additive of organic salts. Scanning electron microscopic (SEM) images show that the products have regular microscopic arrays and layer sheet-like morphology. The disordered mesoporous materials are hydrothermally more stable than highly ordered MCM-41. Furthermore, they show stronger acid strength and higher cracking activities than Al-containing MCM-41.

Keywords: Al-MCM-41; Scanning electron microscope; X-ray diffraction; Mesoporous materials

1. Introduction

The successful synthesis of a new family of mesoporous materials with large surface area, uniform pore size and large pore volume has greatly expanded the capacities of heterogeneous catalysts [1–6,32,33]. However, the surface acid sites including Brönsted and Lewis acid in such Al-containing mesoporous silica materials prepared by amphiphilic surfactant templating are very low even at high aluminum concentration, which limits their applications on the conversion of large molecules [2,3,7]. Therefore, a great effort has been made to increase the acid strength and enlarge the number of acid sites of Al-MCM-41. Borade and Clearfield [8] have reported a synthesis of Al-MCM-41 with Si/Al ratio as low as 2 without observing the presence of octahedral Al. Several post-synthesis routes have also been developed for the preparation of Al-containing MCM-41 [9–11]. Unfortunately, little results show the strong Brönsted acid sites generated on the mesoporous materials. The lack of the strong acidic sites for mesoporous materials is believed to result from amorphous aluminosilicate wall. All attempts to synthesize mesoporous silicates with a crystalline framework were proved to be unsuccessful since the wall thickness for MCM-41 is

* Corresponding author. Tel.: +86-21-6564-2036; fax: +86-21-6564-1740.
E-mail address: dyzhao@fudan.edu.cn (D. Zhao).

0920-5861/01/$ – see front matter
PII: S0920-5861(01)00318-2

too thin. Recently, a family of thick wall mesoporous silica SBA-15 have been successfully synthesized by using amphiphilic triblock copolymers [12,13]. However, Al-SBA-15 could not be directly synthesized and the silicate species were hardly crystallized to form an ordered framework since it was synthesized under strong acid media.

Besides lack of the strong acidity, another disadvantage of Al-MCM-41 is the lack of hydrothermal stability, which would greatly limit its applications in acid catalysis [14]. Upto now, there are several routes related to the improvement on the hydrothermal stability of mesoporous materials, such as pH adjustment [15], salt effect [14], post-treatment with phosphoric acid [16] and thicken the wall [12,13,17]. The hydrothermal stability of MCM-41 is largely improved through these methods. However, the results are still unsatisfactory.

A newly synthesized disordered mesoporous material, which is denoted as KIT-1, has attracted our attention because of its outstanding hydrothermal stability [18]. The KIT-1 mesoporous material was synthesized by hydrothermal polymerization of silicate and aluminate anions surrounding the molecular organization of hexadecyltrimethylammonium chloride in the presence of various organic polyacids. Its channel arrangement interconnects in a three-dimensional disordered way and its structure is stable in boiling water for 48 h. Few syntheses of these disordered mesoporous materials have been reported before [19–21]. The discovery showed a possibility of finding non-crystalline molecular sieves with uniform pore size and excellent hydrothermal stability. Unfortunately, the disordered mesoporous silica KIT-1 must be synthesized with a large amount of organic salts such as NaEDTA (ethylendiamineteraacetic acid disodium) and lack of the strong acidity.

In this paper, we report on a simple synthesis procedure to directly synthesize hydrothermally stable, strong surface acidic, disordered mesoporous aluminosilicates (DMASs) by using cationic surfactant CTAB as the structure-directing agent and the polymer aluminosilicate precursors. The resulted materials show highly hydrothermal stability, furthermore, they show stronger surface acid strength and higher cracking activities than highly ordered Al-containing MCM-41. The disordered mesoporous material is very similar to mesoporous material MCM-41 as regards its uniform mesopore size at the mean value of 3.0 nm, while the mesoporous channel arrangement is disordered similar to that for KIT-1. SEM images show that the products have regular microscopic arrays and layer sheet-like morphology.

2. Experiments

2.1. Synthesis

The disordered mesoporous materials were synthesized from a polymer aluminosilicate precursor prepared according to the procedure previously described [22]. In a typical synthesis, 0.95 g sodium aluminate (4.35 mmol Al_2O_3) was dissolved in 6.5 g 2 M NaOH (13 mmol) and 10.0 g (556 mmol) deionized water, then 15.0 g (100 mmol) LUDOX AS-40 colloidal silica (40 wt.%, Aldrich) was added with strong stirring. After aged at room temperature for 3 days, a solution of 4.44 g (12.2 mmol) CTAB in 60 g (3.33 mol) water was added with stirring. After stirring at room temperature for 3 h, the gel was loaded to an autoclave and heated at certain temperature for 3 days. After cooling to room temperature, the solid products were recovered by filtration, washed with water and dried at room temperature in air. The samples are denoted as DMAS-*X*, where *X* represents for the crystallization temperature (100, 120, 144 and 160°C). Highly ordered pure silica MCM-41 was prepared according to previously described method [23] and tetraethoxysilane (TEOS) as the silica source. Alumination of silica MCM-41 was carried out in dry hexane by using aluminum isopropoxide as the aluminum source [24]. The calcination was carried out in an oven at 550°C in air for 8 h with slow increase of temperature.

2.2. Characterization

Powder X-ray diffraction (XRD) patterns were recorded by a Rigaku D/MAX-IIA X-ray powder diffractometer, and using Ni-filtered Cu Kα radiation and operated at 40 kV and 20 mA.

Surface areas and N_2 adsorption–desorption isotherms for the samples were measured on an ASAP-2010 apparatus using nitrogen as adsorbate at −196°C. The pore size data were analyzed by the BJH method with Halsey equation for multilayer thickness.

Thermogravimetric (TG) analysis was performed on a Rigaku PTC-10A. After flowing Ar gas of 40 ml/min for 2 h, the samples were heated with a heating rate of 10°C/min from room temperature to 850°C.

NH_3-temperature program desorption (NH_3-TPD) was performed on 100 mg of the catalyst with helium (40 ml/min) as the carrier gas and a thermoconductor as the detector. The catalyst was first calcined in helium at 550°C for 1 h and saturated with ammonia at 120°C, then the NH_3-TPD test was started with a heating rate of 15°C/min. In order to reduce the influence of desorption water from the surface hydroxyl group, the amount of desorption ammonia was reanalyzed on a gas chromatograph after the separation of NH_3 with water.

Pyridine adsorption infrared spectra (IR) were obtained on a Nicolet 5SXC FTIR spectrometer. The self-supporting wafers about 5 mg/cm^2 were first evacuated in situ in an IR cell at 350°C for 4 h, and the spectra were recorded after cooling at room temperature. Pyridine was then admitted to desorption at 120, 145, 175, 205, 235, 275 and 300°C.

^{27}Al MAS NMR spectra were recorded at room temperature on a Bruker MSL-300 spectrometer with resonance frequencies of 78.21 MHz [27]. The magnetic field was 7.05 T. The spin rate of the samples was 4.0 kHz and the number of scans was 4000–5000. The pulse lengths were adjusted to 4.6 μs with repetition times to 500 ms. The sweep width was 29477 Hz. External Al-$(H_2O)_6^{3+}$ was used as a reference.

2.3. Catalytic test

The catalytic cracking reactions of *n*-cetane (*n*-C_{16}), *n*-dodecane (*n*-C_{12}) and *n*-heptane (*n*-C_7) were carried out in a pulse microreactor at a H_2 pressure of 2.2 bar and a hydrogen flow rate of 30 ml/min. The catalyst (100 mg) with the particle size of 0.28–0.45 mm was pretreated in situ in a quartz tube with 4 mm i.d. by heating in hydrogen at 500°C for 2 h. The cracking activities were then investigated by the injection of 1 μl of the reactant into the catalyst bed at temperature of 450°C. Reactants and products were analyzed online by a gas chromatograph, equipped with a capillary OV-101 column (50 m length, 0.25 mm i.d.) and with a flame-ionization detector.

3. Results and discussion

DMASs can be directly synthesized by reacting cationic surfactant such as CTAB with the polymerized aluminosilicate precursors [22]. The Si/Al ratio of the polymerized precursors can be varied from 5 to 30 to obtain high crystalline disordered mesoporous aluminosilicates. The precursors have been proved to contain the initial polymerized aluminosilicate species for synthesis of zeolite mordenite [22]. Without CTAB the aluminosilicate precursors are heated at 175°C for 2–3 days, full crystalline mordenite zeolite can be obtained. For comparison, pure silica MCM-41 have been synthesized under base synthesis condition [23] and Al-containing MCM-41 has been prepared by post-treatment procedure and using aluminum isopropoxide as the Al source in dry hexane [24]. XRD patterns for as-synthesized DMAS samples (Fig. 1) show three well-resolved reflection peaks indexed as (1 0 0), (2 0 0) and (3 0 0) at 2θ range of 1–7°, which are similar to that of mesoporous KIT-1. While at high angle of 15–30°, only a very broad diffraction peak caused from amorphous silica wall is observed for all samples, suggesting that no other crystalline phase is formed. Compared with that (d_{100}, 4.0–4.2 nm) for KIT-1 prepared in the presence of organic salts such as EDTA, the as-synthesized DMASs have a larger d_{100} spacing of ~4.98 nm (Table 1). With the increasing synthesis temperature, XRD patterns of DMASs become relatively poorly resolved and the d(1 0 0) spacing increases a little bit (Fig. 1, Table 1). After calcination at 550°C for 8 h, XRD patterns become much better-resolved and the intensities are much increased (Fig. 1), suggesting that the DMASs are thermally stable and further cross-linking of aluminosilicate species is occurred to give better-organization for the mesostructures. It is interesting that the d(1 0 0) spacing is not decreased but a little bit increased after calcination (Table 1), indicating that no structural shrinkage occurs because the inorganic walls may consist of relatively high polymerization aluminosilicate precursors. The relative large precursors can further cross-linked together and reorganized mesostructure. On the other hand, as-synthesized pure silica MCM-41 prepared by using monosilicate TEOS as the silica source and cationic surfactant CTAB as the template without aging under base synthesis condition [23] show well-resolved XRD pattern. Seven diffraction

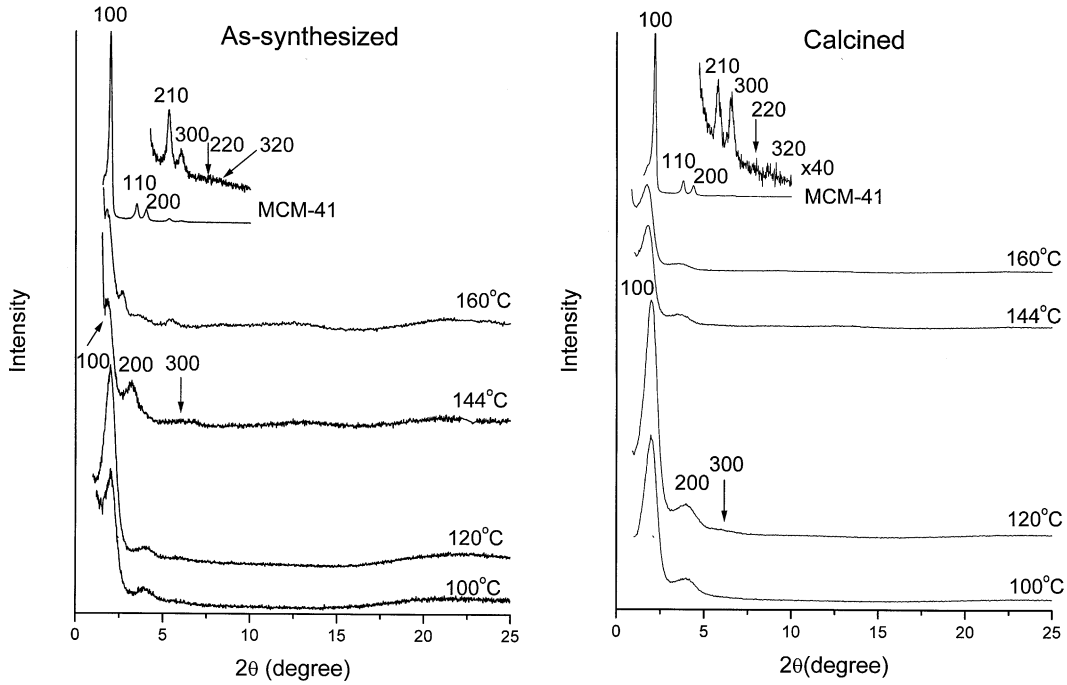

Fig. 1. Powder XRD patterns of as-synthesized, calcined DMASs prepared at different temperatures, and as-prepared and calcined Si-MCM-41.

peaks are observed at 2θ of 1–10°, indicating that the Si-MCM-41 is a high quality mesoporous material. The $d(1\,0\,0)$ spacing of 4.41 nm is a little smaller than that for the DMASs. After calcination, seven diffraction peaks for Si-MCM-41 are retained and the $d(1\,0\,0)$ spacing of 4.01 nm decreases, suggesting that further cross-linking of the silica species to result in shrinking is occurred. Unlike DMAS materials, highly ordered Si-MCM-41 consists of low polymerization silica species on the wall. After alumination in dry hexane, as-prepared and calcined Al-MCM-41 show similar XRD patterns (not shown) except the intensities and the d spacing a little bit decrease (Table 1), indicating that Al-MCM-41 have highly ordered mesostructure.

Transmission electron microscopy (TEM) image of calcined DMAS (Fig. 2a) shows full-disordered mesostructure but with relatively uniform mesopore, further confirming that calcined DMAS samples have

Table 1
The physical properties of the disordered mesoporous materials and Al-MCM-41

Sample	Si/Al ratio	$d(1\,0\,0)$ (nm)		N_2adsorption data			Total weight loss (wt.%)	Amount of desorption NH_3 (mmol/g)[a]
		As-made	Calcined	Pore size (nm)	BET surface area (m^2/g)	Pore volume (ml/g)		
DMAX-100	18	4.98	5.11	2.9	610	0.64	49	0.40
DMAX-120		4.94	4.95	2.9	450	0.50	44	0.36
DMAX-144	22	4.55	4.58	2.9	445	0.45	43	0.32
DMAX-160		4.51	4.52	3.0	380	0.40	39	0.29
MCM-41		4.41	4.01	2.2	1130	0.67	44	
Al-MCM-41	14	4.35	3.94	2.1	790	0.47		0.16

[a] The amount of desorption ammonia was re-analyzed on a gas chromatograph after separation of NH_3 with water.

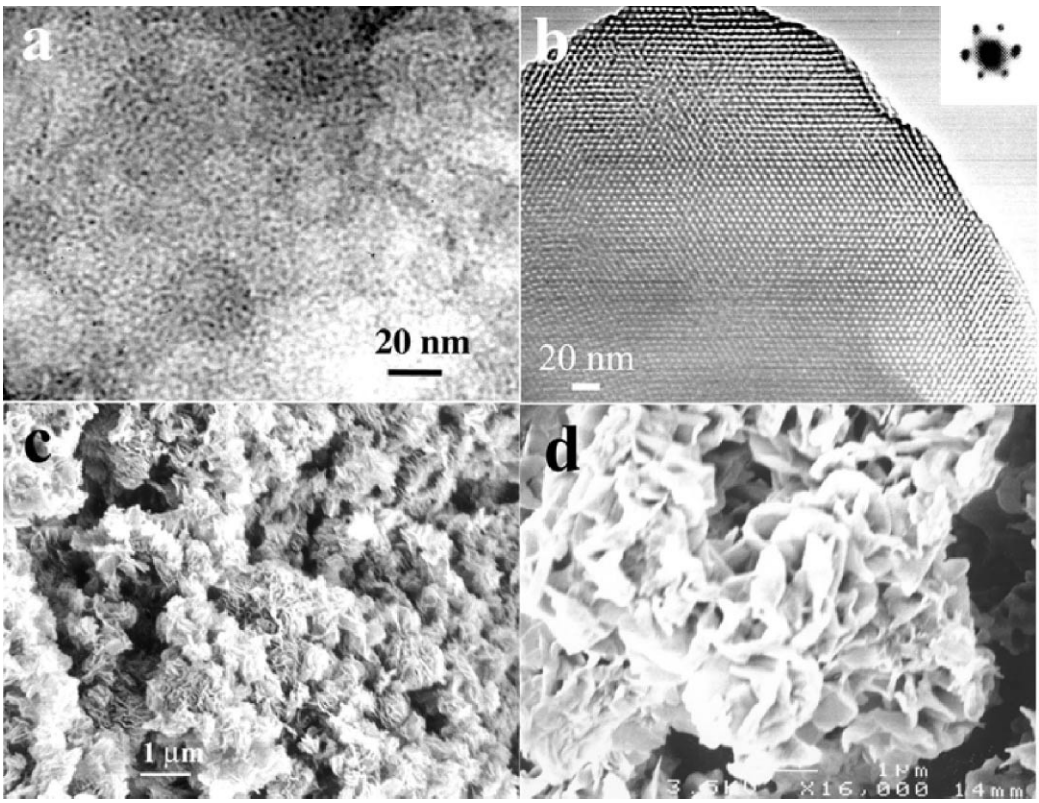

Fig. 2. TEM images of: (a) DMAS prepared at 100°C; (b) highly ordered pure silica MCM-41 and SEM images; (c, d) DMASs with different magnification.

fully disordered mesostructures similar to that for KIT-1. The selected electron diffraction of calcined samples does not show that the wall of DMAS has regular ordered array, suggesting that the inorganic wall consists of amorphous aluminosilicates. On the other hand, calcined Si-MCM-41 shows well-ordered two-dimensional hexagonal mesostructrue (Fig. 2b), further confirming that it is a high quality mesoporous molecular sieve. After alumination, TEM measurement shows that Al-MCM-41 retains highly ordered mesostructure, suggesting that the alumination process in dry hexane does not affect the organization of the mesoporous materials. SEM images (Fig. 2c and d) for as-synthesized DMAS samples have microscopically regular array of layer sheet-like similar to the morphology of MCM-22 [25,34]. After calcination at 550°C for 8 h, layer-sheet-like morphology is retained, suggesting that the structure is stable. While SEM images show that the highly ordered Si-MCM-41 prepared by using CTAB as the templates under base synthesis condition and Al-MCM-41 have agglomerated particles (∼2μm), suggesting that they have do not regular macroscopical ordering.

The calcined DMAS materials have significantly greater hydrothermal stability in comparison to calcined highly ordered Si-MCM-41 material prepared by using cationic surfactant CTAB as the template in base synthesis condition. All of the calcined DMAS samples prepared with the polymer aluminosilicate precursors are stable after heating in boiling water for more than 70 h. For example, the XRD pattern of calcined DMAS-100 prepared at 100°C is essentially unchanged from that obtained after the sample has been heated in boiling water for 24 h (Fig. 3A). All scattering reflections are retained after this hydrothermal treatment, although the (3 0 0) reflection peak becomes broader. The (1 0 0) peak, however, is observed with similar intensity (Fig. 3A). Even after heating in

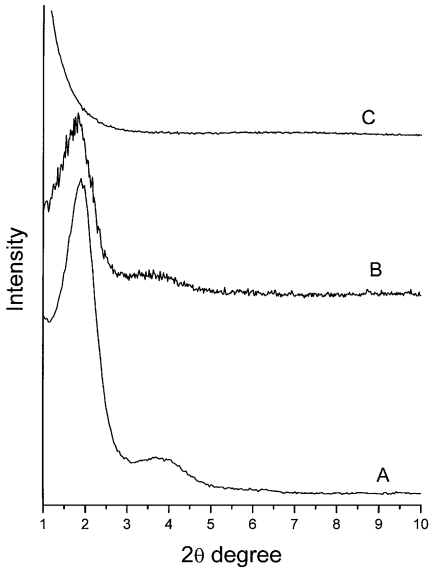

Fig. 3. Powder XRD patterns of calcined DMAS-100 after heating in boiling water for: (A) 12 h, (B) 70 h, (C) calcined pure silica MCM-41 after heating in boiling water for 6 h.

boiling water for 70 h, the (1 0 0), (2 0 0) diffraction peaks are still retained, and the intensities are a little decreased (Fig. 3B). In contrast to this, the calcined highly ordered Si-MCM-41 prepared by using cationic surfactant CTAB under base synthesis condition is unstable, after heating in boiling water for 6 h, the material becomes amorphous and loses all XRD scattering reflections (Fig. 3C) [12,18]. In addition, mesoporous aluminosilicate material AlHMS with Si/Al ratio of 15 prepared by using hexadecylamine [26] is stable after heating treatment at 90°C water for 6 h, but longer time of the boiling water treatment results in the significant decrease of the XRD intensity and surface area and pore volume for the AlHMS sample, which shows similar stability to that of Al-MCM-41 with the same Si/Al ratio [26], suggesting that hydrothermal stability of the disordered aluminosilicates DMAX are also higher than that of AlHMS.

The TG analysis measurements show total weight loss of 39–49 wt.% for DMAS samples, which due to the removal of organic templates of CTAB [27]. The results are similar to that (44 wt.%) (Table 1) for Si-MCM-41 and almost all of the templates can be removed after calcination at 550°C for 8 h.

Representative nitrogen adsorption/desorption isotherms and the corresponding pore size distribution

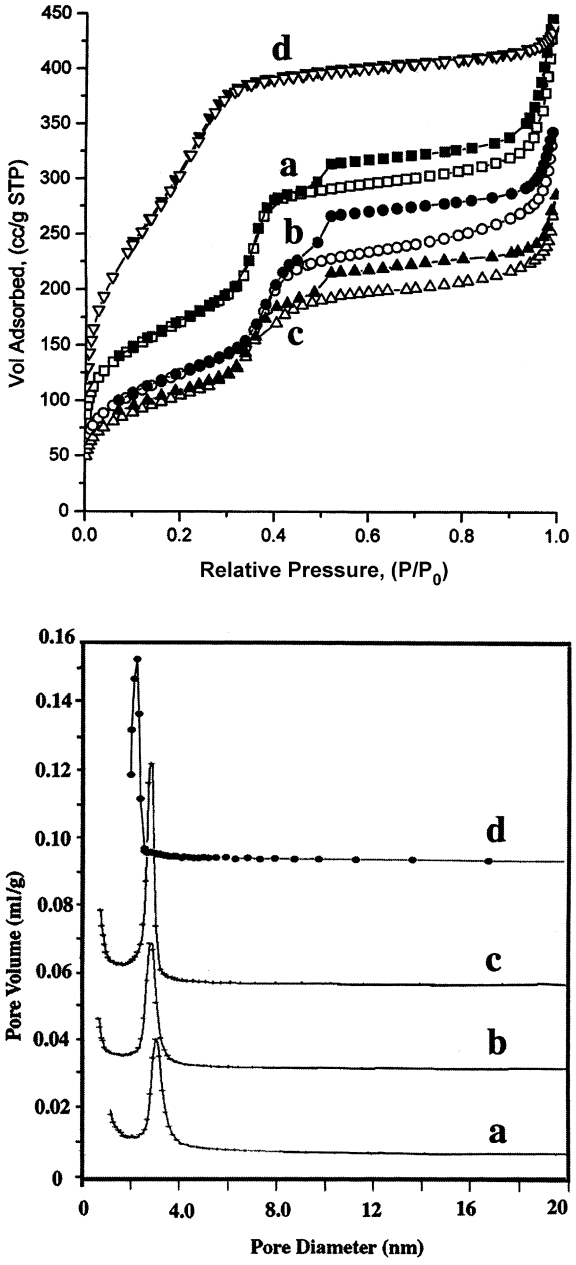

Fig. 4. N_2 adsorption/desorption isotherms (up) and pore size distribution (down) calculated based on BJH model from adsorption branches for a, b, and c, DMASs prepared at different temperature of (a) 100°C; (b) 120°C; (c) 144°C; (d) calcined MCM-41.

calculated by BJH model from adsorption branch are shown in Fig. 4. Calcined DMASs prepared from the polymerized aluminosilicate precursors yield the

complex type isotherms. A steep increase is observed at a relative pressure at $0.32 < P/P_0 < 0.5$, which is due to the filling of mesopores by capillary condensation [13,28]. Another step is observed in the adsorption curve at a relative pressure 0.95–1.0, which may be due to the filling of the macropore caused from the void space between the sheet-like crystals [29]. All samples show narrow pore size distribution at the mean values of ~3.0 nm (Fig. 4, Table 1), suggesting that the DMASs prepared directly from the polymer precursors have well-uniformed mesoporous channels. With the increase of synthesis temperature, the BET surface area for disordered mesoporous materials decreases, but the pore size is always kept constant (Table 1). While, highly ordered Si-MCM-41 shows a typical I–V isotherm curve without hysteresis and the capillary condensation occurs at a lower relative pressure ($P/P_0 \sim 0.10$–0.30) (Fig. 4d). The corresponding pore size distribution calculated from adsorption branch (Fig. 4d) [30] shows a narrower distribution peak at the mean values of 2.2 nm than those for the DMASs. The BET surface areas for Si-MCM-41 is 1130 m^2/g much higher than those for DMAS samples. After alumination, the BET surface area and pore volume a little decrease, but still higher than those for DMAS materials prepared directly from the polymer aluminosilicate precursors.

Fig. 5 shows the ^{27}Al-MAS NMR spectra of as-synthesized and calcined DMASs prepared from the polymer aluminosilicate precursors at 100 and 144°C, respectively. All spectra give two resolved lines at 55 and 0 ppm. The line at 55 ppm can be assigned to the aluminum in a tetrahedral environment (AlO_4), in which aluminum is covalently bound to four Si atoms via oxygen bridges, whereas the chemical shift at 0 ppm can be assigned to octahedral aluminum (AlO_6) [24]. The results clearly show that almost all of aluminum for as-synthesized DMAS-100 are in the presence of AlO_4 structure unit (Fig. 5). After calcination at 550°C in air the intensity of the line at 0 ppm increases (Fig. 5), suggesting that some of aluminum with AlO_4 unit, which are located on the framework of the disordered mesoporous materials are unstable and can be moved out from the framework to become non-framework octahedral aluminum AlO_6. Compared with those for as-synthesized and calcined samples prepared at 144°C, as-synthesized and calcined DMAS-100 samples show lower intensities corresponding to the line at 0 ppm (Fig. 5), indicating that lower synthesis temperature enhances the incorporation of aluminum into the mesoporous materials framework, which is in agreement with the XRD data. As shown in Fig. 5, as-prepared highly ordered Al-MCM-41 shows only one line at 50 ppm, indicating that the simple post-alumination process can result in all the aluminum located on the frameworks of MCM-41. After calcination at 500°C for 8 h in air, a weak line at 0 ppm is observed (Fig. 5), suggesting that a little dealumination occurs during the calcination. Compared to Al-MCM-41, aluminum located on the frameworks of the DMAS prepared at low temperature such as DMAS-100 is more stable, while the aluminum on DMASs prepared at high temperature is less stable.

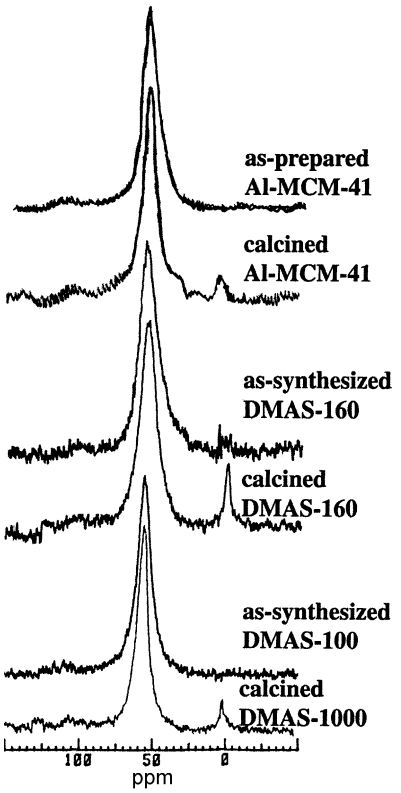

Fig. 5. ^{27}Al-MAS NMR spectra of as-synthesized and calcined DMASs prepared at 100 and 144°C respectively; and as-prepared and calcined Al-MCM-41 prepared by post-synthesis of MCM-41 with aluminum isopropoxide in dry hexane.

^{29}Si-MAS NMR spectra of as-synthesized and calcined DMASs prepared at 100 and 144°C show

the broad lines at 110 ppm resulted from the silicon associated with proton and aluminum, further indicating that the wall for the samples are amorphous aluminosilicates [12,13,29]. The lines at 110 ppm for the samples prepared at 144°C are much broader than those for the sample prepared at 100°C, suggesting that higher synthesis temperature yield a more disordered wall [2,14]. As-synthesized pure Si-MCM-41 shows three relative narrow lines at 93, 100 and 110 ppm, which correspond to Q^2, Q^3 and Q^4 silica species, respectively, associated with progressively increased silica cross-linking. From the relative peak areas, the ratios of these species are established to be $Q^2{:}Q^3{:}Q^4 = 0.04{:}1{:}0.8$. After calcination at 550°C, the Q^4 line increases and the ratio becomes $Q^2{:}Q^3{:}Q^4 = 0.04{:}0.67{:}1$, indicating that further cross-linking occurs and condensed amorphous silica framework is formed during the calcination. After alumination, the line at 110 ppm becomes broad, which is caused from aluminum. Compared with the DMASs, Al-MCM-41 shows a broader line around 110 ppm, suggesting that highly ordered Al-MCM-41 may have more disordered wall structure [2,14].

4. Acid properties

Fig. 6 shows TPD of ammonia (NH_3-TPD) curves on calcined DMAS materials and Al-containing MCM-41 with similar Si/Al ratio, respectively. Obviously, the desorption temperature and amount of ammonia for all calcined DMAS samples are higher than those for Al-MCM-41 with similar Si/Al ratio (Table 1). Two desorption peaks that may cause from weak and strong surface acidity, respectively, can be observed for calcined DMAS materials prepared at 100 and 120°C (Fig. 6a), although latter peaks do not go down to the base line, which may cause from further desorption of the hydroxyl groups from the mesoporous materials. In order to accurately calculate the desorption amount of the ammonia, we have separated the ammonia with the water from desorption of the hydroxyl groups on the mesoporous materials, and analyzed it again in gas chromatograph (see Table 1). These results suggest that DMASs prepared at low temperature have more acidic sites than that for Al-MCM-41 with similar Si/Al ratio. With increasing synthesis temperature, the desorption amount of ammonia decreases and high temperature desorption peak becomes poorly resolved (Fig. 6b), suggesting that low temperature synthesis may yield large amount of the surface acidic sites.

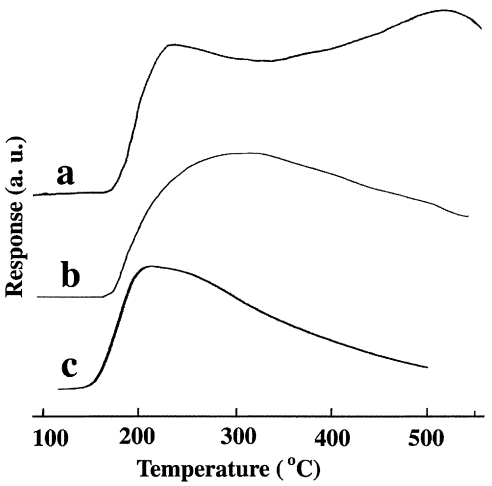

Fig. 6. NH_3-TPD profiles for (a) DMAS prepared at 100°C; (b) DMAS prepared at 144°C; (c) calcined Al-MCM-41.

IR spectra of pyridine adsorption on calcined DMASs and Al-MCM-41 with similar Si/Al ratio are shown in Fig. 7. It is clear that both Brönsted (band at 1540 cm^{-1}) and Lewis (band at 1450 cm^{-1}) acid sites can be observed on these samples [31]. IR spectra show that the calcined DMASs especially DMAS-100 has a larger amount of Brönsted acid sites than that for Al-MCM-41, suggesting that DMAS samples prepared directly from the polymer precursors yield more surface acid sites than that for Al-MCM-41. Moreover, after degassed at 250°C, the 1540 cm^{-1} peak associated with Brönsted acid sites totally disappears on the Al-MCM-41, whereas it still remains on the DMAS-100 sample even after desorption at 300°C, indicating that the strength of Brönsted acid sites on DMAS-100 sample is stronger than that on the Al-MCM-41. The results indicate that DMAS materials prepared directly from the polymer precursors have medium strength Brönsted acid sites, which are much stronger than that for highly ordered Al-MCM-41 with similar Si/Al ratio. Moreover, mesoporous AlHMS with the Si/Al ratio of 15 prepared by using hexadecylamine as a structure-directing agent shows similar acidity to Al-MCM-41 [26],suggesting that the strength of

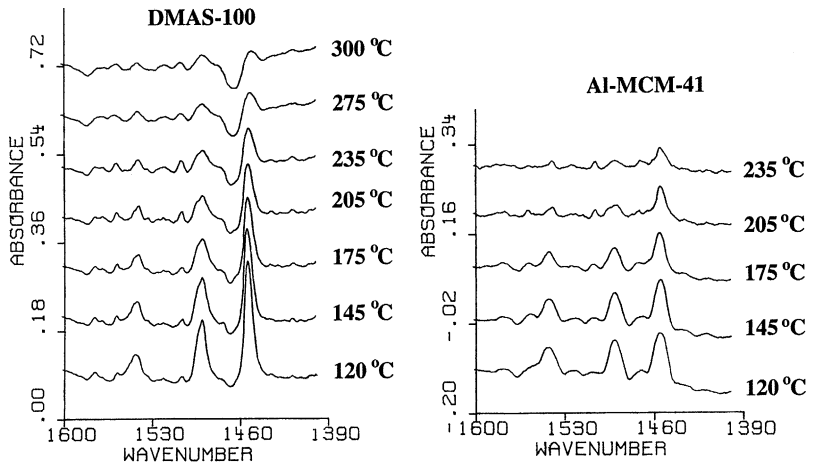

Fig. 7. IR spectra of pyridine adsorbed on DMAS prepared at 100°C and Al-MCM-41 and degassed at different temperature.

Table 2
The cracking activity of disordered and Al-MCM-41 mesoporous materials

Sample	Conversion (%)			C (C_{12})/C (C_{16})[a]	C (C_7)/C (C_{16})[b]
	n-C_{16}	*n*-C_{12}	*n*-C_7		
DMAS-100	82.2	17.4	3.6	0.21	0.044
DMAS-144	77.8	14.6	2.9	0.19	0.037
Al-MCM-41	60.1	7.8	0.6	0.13	0.001

[a] Representing the ratio of *n*-C_{12} conversion to *n*-C_{16}'s.
[b] Representing the ratio of *n*-C_7 conversion to *n*-C_{16}'s.

Brönsted acid sites on the DMASs is also stronger than that on AlHMS.

5. Catalytic activity

The catalytic activities of the DMAS samples towards cracking of *n*-alkanes are illustrated in Table 2. Generally speaking, the cracking of *n*-alkanes with short alkyl chains needs the catalysts with strong acid sites. Therefore, we choose *n*-alkanes with different long alkyl chains as the reactants to study the acid strength for the samples. As shown in Table 2, the DMAS samples exhibit good activities for *n*-C_{16} cracking, but for *n*-alkanes with short alkyl chains the cracking activities decrease greatly. The results indicate that the acid strengths of the DMAS samples are mild. Meanwhile, for cracking reactions of all *n*-alkanes the activities decrease in order: DMAS-100 > DMAS-144 > Al-MCM-41. This may result from the different number and strength of acid sites. The acid strength of these samples can be described more clearly by using the ratio of *n*-C_{12}'s conversion to *n*-C_{16}'s or *n*-C_7's conversion to *n*-C_{16}'s. As shown in Table 2, the ratio is in the order: DMAS-100 > DMAS-144 ≫ Al-MCM-41, which is in the agreement with the order of acid strength for these samples. These results indicate that the disordered mesoporous materials synthesized directly from the polymer precursors have larger amount of acid sites, stronger acid strength, and therefore higher cracking activity than those for conventional Al-MCM-41 mesoporous material.

Acknowledgements

This work was supported by the National Science Foundations of China (Grant No. 29873012 and 29925309), National Education Ministry and the

Key Laboratory of Chemical Engineering and Technology of Jiangsu Province. We thank Prof. Z. Xue, Mrs. H. Chen and H. Jiang for NMR, IR, TPD, TGA measurements.

References

[1] C.T. Kresge, M.E. Leonowicz, W.J. Roth, J.C. Vartuli, J.S. Beck, Nature 359 (1992) 710.
[2] A. Corma, V. Fornes, M.T. Navarro, J. Perez-Pariente, J. Catal. 148 (1994) 569.
[3] R. Mokaya, W. Jones, Z. Luan, M.D. Alba, J. Klinnowski, Catal. Lett. 37 (1996) 113.
[4] S. Mann, G.A. Ozin, Nature 382 (1996) 313.
[5] D. Zhao, P. Yang, Q. Huo, B.F. Chmelka, G.D. Stucky, Curr. Opin. Solid Mater. Sci. 3 (1998) 111.
[6] H. Yang, N. Coombs, G.A. Ozin, Nature 386 (1997) 692.
[7] J. Weglarski, J. Datka, H.Y. He, J. Klinnowski, J. Chem. Soc., Faraday Trans. 91 (1995) 2995.
[8] R.B. Borade, A. Clearfield, Catal. Lett. 31 (1995) 267.
[9] R. Ryoo, S. Jun, J.M. Kim, Chem. Commun. (1997) 2225.
[10] R. Mokaya, W. Jones, Chem. Commun. (1997) 2185.
[11] H. Hamdan, S. Endud, H. He, M.N.M. Muhid, J. Klinowski, J. Chem. Soc., Faraday Trans. 92 (1996) 2331.
[12] D. Zhao, J. Feng, Q. Huo, N. Melosh, G.H. Fredrickson, B.F. Chmelka, G.D. Stucky, Science 279 (1998) 548.
[13] D. Zhao, Q. Huo, J. Feng, B.F. Chmelka, G.D. Stucky, J. Am. Chem. Soc. 120 (1998) 6024.
[14] R. Ryoo, S. Jun, J. Phys. Chem. 101 (1997) 317.
[15] R. Ryoo, J.M. Kim, Chem. Commun. (1995) 711.
[16] L. Huang, Q. Li, Chem. Lett. (1999) 829.
[17] C. Yu, Y. Yu, D. Zhao, Chem. Commun. (2000) 575.
[18] J.M. Kim, C.H. Ko, C.H. Shin, R. Ryoo, J. Phys. Chem. 99 (1995) 16742.
[19] C. Chen, S. Xiao, M.E. Davis, Micropor. Mater. 4 (1995) 1.
[20] S.A. Bagshaw, E. Prouzet, T.J. Pinnavaia, Science 269 (1995) 1242.
[21] C.J. Guo, Stud. Surf. Sci. Catal. 97 (1995) 165.
[22] Z. Hurem, D. Vucelic, V. Markovic, Zeolites 13 (1993) 145.
[23] Q. Huo, D.I. Margolese, U. Ciesla, D.G. Demuth, P. Feng, T.E. Gier, P. Sieger, A. Firouzi, B.F. Chmelka, F. Schüth, G.D. Stucky, Chem. Mater. 6 (1994) 1176.
[24] Z. Luan, M. Hartmann, D. Zhao, W. Zhou, L. Kevan, Chem. Mater. 11 (1999) 1621.
[25] G.J. Kennedy, S.L. Lawton, M.K. Rubin, J. Am. Chem. Soc. 116 (1994) 11000.
[26] Y. Yue, Y. Sun, Q. Xu, Z. Gao, Appl. Catal. 175 (1998) 131.
[27] C. Chen, H. Li, M.E. Davis, Micropor. Mater. 2 (1993) 17.
[28] D. Zhao, J. Sun, Q. Li, G.D. Stucky, Chem. Mater. 12 (2000) 275.
[29] Q. Luo, L. Li, B. Yang, D. Zhao, Chem. Lett. 11 (2000) 256.
[30] W. Luckens Jr., P. Schmidt-Winkel, D. Zhao, J. Feng, G.D. Stucky, Langmuir 15 (1999) 5403.
[31] X. Chen, L. Huang, G. Ding, Q. Li, Catal. Lett. 44 (1997) 123.
[32] M. Trau, N. Yao, E. Kim, Y. Xia, G.M. Whitesides, I.A. Aksay, Nature 390 (1997) 674.
[33] G.A. Ozin, H. Yang, I. Sokolov, N. Coombs, Adv. Mater. 9 (1997) 662.
[34] S. Nicolopoulos, J.M. Gonzalezcalbet, M. Valletregi, A. Corma, J. Am. Chem. Soc. 117 (1995) 8947.